

Scope. We introduce an approach to model the effects of a combinatorial and sparse space of intervention sequences, including the bursts of non-stationarity that the application of an intervention brings in. We consider the case where each D_n^t behaves as if it was randomized to focus on predictive guarantees on large, possibly underspecified, sequential action spaces. We will consider neither experimental design nor reinforcement learning, instead focusing on the problem of behavioral forecasting under hypothetical future interventions given past controlled interventions.

Challenges and prior work. Much of the sequential intervention literature in AI and statistics considers generic models¹ to map sequences $D_n^{1:t} := [D_n^1, D_n^2, \dots, D_n^t]$ to behavior X_n^t and beyond, sometimes exploiting strong Markovian assumptions or short sequences and small action spaces [Chakraborty and Moodie, 2013, Sutton and Barto, 2018]. An unstructured black-box for sequences, such as recurrent neural networks and their variants [e.g. Hochreiter and Schmidhuber, 1997, Cho et al., 2014, Vaswani et al., 2017], can learn to map a sequence to a prediction. This is less suitable when interventions are categorical and sparse, with most entries corresponding to some baseline category of “no changes”. That is, there is no obvious choice of smoothing or interpolation criteria to generalize from seen to unseen strings $D_n^{1:T}$, with the practical assumption being that we see enough variability to reliably perform this interpolation. There is an increased awareness of problems posed by large discrete spaces among pre-treatment covariates [Yao et al., 2019, Zeng et al., 2024], which is of a different nature as losses can be minimized with respect to an existing natural distribution, as opposed to the interventional problem where the design variables are allowed to be chosen and so sparsity conditions can easily result in very atypical test cases of interest. Several papers address large intervention spaces (mostly for non-sequential problems) without particular concerns about non-smooth, combinatorial identifiability [Kaddour et al., 2021, Nabi et al., 2022, Saito et al., 2023, 2024]. A few more recent papers address explicit assumptions of identifiability directly in combinatorial categorical spaces by sparse regression [Agarwal et al., 2023a] or energy functions Bravo-Hermesdorff et al. [2023], but without a longitudinal component. More classically, tools like the do-calculus [Pearl, 2009] and their extensions [Correa and Bareinboim, 2020] can be used with directed acyclic graphs (DAGs) to infer combinatorial effects, although they often restrict each intervention variable to target a single random variable (e.g. Aglietti et al. [2020]). With strong assumptions and computation, this may include latent variables Zhang et al. [2023]. Alternative representation learning ideas for carefully extrapolating to unseen interventions are presented by [Saengkhyongam et al., 2024] in the non-sequential setting.

In this paper, we consider the conservative problem of *identification guarantees* for the effect of sequential combinations of interventions which may never have co-occurred jointly in training data, *formalizing assumptions* that allows for the transfer and recombination of information learned across units. These are not of the same nature as identifiability of causal effects from observational data [Pearl, 2009] or causal discovery [Spirtes et al., 2000], but of *causal extrapolation*: even in the randomized (or unconfounded) regime, it is not a given that the distribution of a particular potential outcome $X(d^{1:t})$ can be reliably inferred from limited past combinations of interventions without an explicit structure on the causal generative model. We will consider the case where interventions have non-stationary effects: once unit n is exposed to $D_n^t = d_n^t$, then $X_n^{t+\Delta}$ will have dynamics that can be affected not only by the choice of d_n^t but also the difference Δ , resulting in dense dependency structures such as the one in Figure 1. As multiple treatments are applied to the same unit n , there will be a *composition* of effects that will depend not only on the labels of the interventions, but also on the order by which they take place. If a substantive number of choices of interventions at time t is available, a large dataset may have no two sequences $D_n^{1:T}$ and $D_{n'}^{1:T}$ taking the same values, even when considering only the unique treatment values applied n and n' regardless of ordering and time stamps.

Problem statement. Let each individual unit n be described by time-invariant features Z_n and a pair of time-series $(\{X_n^t\}, \{D_n^t\})$. Each D_n^t is a categorical variable representing an *intervention* (also called *treatment*, or *exposure*), encoded by values in \mathbb{N} , and sequentially unconfounded with the system by randomization or assumption. D_n^t describes an intervention which causes changes to the distribution of $X_n^{t:\infty}$, the time-series of state variables starting at time t . The special value $D_n^t = 0$ denotes an “idle” or “default” treatment that can be interpreted as “no intervention”. Given a training set of units $(Z_n, \{X_n^t\}, \{D_n^t\})$ and observations up to a time point T , the goal is to predict future sequence of states for an unit n^* under a hypothetical intervention D_{n^*} . We denote it as $X_{n^*}^{T+1:T+\Delta}(d_{n^*}^{1:T+\Delta})$, where $V^{t_1:t_2}$ denotes a slice of a discrete-time time series of random vectors V from t_1 to t_2 , inclusive; $V(d^{1:t})$ is the potential outcome [Imbens and Rubin, 2015, Hernán and J, 2020, Pearl, 2009] of variable V under interventions $D^1 = d^1, D^2 = d^2, \dots, D^t = d^t$. This process takes place under stable unit treatment value assumption (SUTVA) [Imbens and Rubin, 2015], meaning that interventions D_n^t only affect unit n .

Each intervention D_n^t is allowed to have an impact on the whole future series $t, t+1, t+2, \dots$. It can correspond to an instantaneous shock (“give five dollars of credit at time t ”) or an action that takes place over an extended period of time (“promote this podcast from time t to time $t+5$ ”): we just assume the meaning to be directly encoded within

¹We include here models which explicit parameterize causal contrasts in longitudinal interventions, such as the blip models of Robins [1997].

arbitrary category labels $0, 1, 2, 3, \dots$. In a real-world scenario where a same action can be applied more than once, different symbols in \mathbb{N} should be used for each instance (e.g., 1 arbitrarily standing for “give five dollars”, and 2 for “give five dollars a second time” and so on).

In Section 2, we provide an account of what we mean by compositionality of interventions, with explicit assumptions for identifiability. In Section 3, we describe an algorithm for likelihood-based learning, along with approaches for predictive uncertainty quantification. Further related work is covered in Section 4 before we perform experiments in Section 5, highlighting the shortcomings of black-box alternatives.

2 A Structural Approach for Intervention Composition

For simplicity, we will assume scalar behavioral measurements X_n^t , as the multivariate case readily follows. Consider the following conditional mean model for the potential outcome $X_n^t(d_n^{1:t})$,

$$\mathbb{E}[X_n^t(d_n^{1:t}) \mid x_n^{1:t-1}(d_n^{1:t-1}), z_n] = (\phi_n^t)^\top (\beta_n \odot \psi_n^t) = \sum_{l=1}^r \phi_{nl}^t \beta_{nl} \psi_{nl}^t, \quad (1)$$

where \odot is the elementwise product, $X_n^t(d_n^{1:t'}) = X_n^t(d_n^{1:t})$ for any $t' \geq t$ (future interventions do not affect past outcomes), and $Z_n(d_n^{1:t}) = Z_n$ for all t . We do not explicitly condition on $D_n^{1:t}$ in most of our notation, adopting a convention where potential outcome indices $d_n^{1:t}$ are always in agreement with the (implicit) corresponding observed $D_n^{1:t}$. We define $\phi_{nl}^t := \phi_l(x_n^{1:t-1}(d_n^{1:t-1}), z_n)$ as evaluations of basis functions $\phi_l(\cdot)$, which for now we will assume to be known. Each individual n has their individual-level coefficients β_n . Causal impact, as attributed to $D_n^{1:t} = d_n^{1:t}$, is given by

$$\psi_{nl}^t := \prod_{t'=1}^t \psi_l(d_n^{t'}, t', t), \quad (2)$$

where function $\psi_l(d, t', t)$ captures a trajectory in time for the effect of $D_n^{t'} = d$, for $t' < t$. We consider two variants. The first is a *time-bounded* variant which, for $d > 0$, defines $\psi_l(d, t', t) := w_{dl, t-t'}$, where $w_{dl, t-t'}$ is a free parameter for $0 \leq t - t' < k_d$, otherwise $w_{dl, t-t'} = w_{dl, k_d-1}$. The intuition is that the effect of intervention level d has no shape constraints but it cannot affect the past and it must settle to a constant after a chosen time window hyperparameter $k_d > 0$. The default level $d = 0$ has no effect and no free parameters, with $\psi_l(0, t', t) = 1$. The second variant is motivated by real-world phenomena where causal impacts diminish their influence over time and result in a new equilibrium [Brodersen et al., 2015]. We consider a *time-unbounded* shape with exponential decay, parameterized as

$$\psi_l(d, t', t) := \sigma(w_{1dl})^{t-t'} \times w_{2dl} + w_{3dl}, \quad (3)$$

where $\sigma(\cdot)$ is the sigmoid function, so that $0 < \sigma(w_{1dl}) < 1$. As t grows, $\sigma(w_{1dl})^{t-t'}$ goes to 0. w_{3dl} is the stationary contribution of an intervention at level d . In particular, for $d = 0$, we define $w_{10l} = w_{20l} = 0$ and $w_{30l} = 1$, while for $d > 0$ we have that w_{1dl} , w_{2dl} and w_{3dl} are free parameters to be learned. By defining k_d as the *dimensionality of intervention level d* , we adopt the convention $k_d = 3$ for the prescribed time-unbounded model of Eq. (3).

2.1 Representation Power and Compositional Warping

Eq. (1) is reminiscent of tensor factorization and its uses in causal modeling [Athey et al., 2021, Agarwal et al., 2023b], where the primary motivation comes from the imputation of missing potential outcomes taking place on a pre-determined period in the past. From a predictive perspective, it can be motivated from known results in functional analysis (such as Proposition 1 of [Kaddour et al., 2021]) that allows us to represent a function $f(x)$ by first partitioning its input into (x_a, x_b) and controlling the approximation error given by an inner product of vector-valued functions $f(x_a, x_b) \approx f_a^\top(x_a) f_b(x_b)$, in practice choosing the dimensionality of the vectors by a data-driven approach. Although those results apply typically to smooth functions with continuous inputs (such as the Taylor series approximation, which relies on vectors of monomials with coefficients constructed from derivatives), discrete inputs such as e.g. $D_n^{1:T}$ at a fixed dimensionality T can be separated from the other inputs as $f(n, d^{1:T}, x^{1:T}, z) = f_d^\top(d^{1:T}) f_{n,xz}(n, x^{1:T}, z)$. Here, similarly to classical ANOVA models, $f_d(\cdot)$ is a one-hot encoding vector for the entire (exponentially sized) space of possible $d_n^{1:T}$ trajectories, and $f_{n,xz}(\cdot, \cdot, \cdot)$ returns a vector of corresponding length.

As we do not want to restrict ourselves to fixed T (and N), not to mention an exponential cost of representation, we will resort to fixed-dimensional embeddings of sequences and identities. In particular, we design $f_d(d^{1:t})$ to have a finite output dimensionality r_g . Inspired by sequential hidden representation models such as recurrent neural networks, we define $f_{dl}(d^{1:t}) := g_l(d^{1:t}, t, t)$, for $l \in 1, 2, \dots, r_g$, via the following recursive definition on $0 \leq t' \leq t$:

$$g_l(d^{1:t'}, t', t) := h_l(g_l(d^{1:t'-1}, t' - 1, t), d^{t'}, t', t), \quad (4)$$

such that $h_l(v, 0, t', t) \equiv v$ for any (v, t', t) (that is, intervention level $D_n^{t'} = 0$ does nothing) and $h_l(v, d, 0, t) \equiv 1$ for any (d, v, t) (base case). A representational choice $h_l(v, d, t', t) := h_{l_1}(v)^\top h_{l_2}(d, t', t)$ requires a choice of dimensionality r_{h_l} for the inner vectors h_{l_1}, h_{l_2} . Recursively applying (4) in this product form can still be done relatively efficiently, but choosing $r_{h_l} = 1$ for all l simplifies matters as we apply again the inner product formula to $f_d^\top(d^{1:T})f_{nxz}(n, x^{1:T}, z)$ to get to a factorization form analogous to Eq. (1). More formally:

Proposition 1 *Let $f(n, d^{1:T}, x^{1:T}, z) := f_d^\top(d^{1:T})f_{nxz}(n, x^{1:T}, z)$, where function sequences $f_d(d^{1:T})$ and $f_{nxz}(n, x^{1:T}, z)$ are defined for all $T \in \mathbb{N}^+$ and have codomain \mathbb{R}^{r_g} . Furthermore, define $f_{dl}(d^{1:T})$ as in Eq. (4) with $r_h = 1$, and the l -th entry of $f_{nxz}(n, x^{1:T}, z)$ as $f_{nxzl}(n, x^{1:T}, z) := u_l(n)^\top v_l(x^{1:T}, z)$, each of the latter having codomain $\mathbb{R}^{r_{s'}}$ and where $v_l(\cdot, \cdot)$ is defined recursively for any T , similarly $g_l(\cdot, \cdot, \cdot)$. Then there exists some integer r and three functions a, b and c with codomain \mathbb{R}^r so that $f(n, d^{1:T}, x^{1:T}, z) = \sum_{l=1}^r a_l(n) \times b_l(x^{1:T}, z) \times c_l(d^{1:T}, T)$. Moreover $c_l(d^{1:T}, T) = \prod_{t=1}^T m_l(d^t, t, T)$ for functions $m_l : \mathbb{N}^3 \rightarrow \mathbb{R}$.*

Proofs of this and next results are given in Appendix B. The above shows that if we start with an assumption that the ground truth function takes some desired form, then there is some finite r_g for which our combination of basis functions can parameterize the ground truth function for arbitrary T , analogous to in Eq. (1). On the other hand, we show a companion result below, that if we hold T fixed, there is some fixed value for r_g , which depends polynomially on T , such that any measurable ground truth function can be approximated by our combination of some appropriate choice of basis functions. This is reminiscent of the line of work on matrix factorization (e.g., Appendix A of Agarwal et al. [2023c]).

Proposition 2 *Given a fixed value of T , suppose we have a measurable function $f : \bigcup_{t=2}^T \mathcal{X}^{1:t-1} \times \bigcup_{t=1}^T \mathcal{D}^t \times \mathcal{Z} \rightarrow \mathbb{R}^d$, $t \leq T$, where $\mathcal{X}^{1:t-1}$ and \mathcal{Z} are compact, \mathcal{D}^t is finite. For $d = 1, \dots, d_{max}$, let $m_d : \bigcup_{t=1}^T \mathcal{D}^t \rightarrow \{1, \dots, T\}$ with $m_d(\mathbf{d}) = t$ if $\exists t$ s.t. $\mathbf{d}_t = d$ else 0. For every T there exist $r_g = O(T^{d_{max}+1})$ such that for any ϵ , there are measurable functions $\phi_l : \mathcal{X}^{1:t-1} \times \mathcal{Z} \rightarrow \mathbb{R}^d$ and $\psi_{ld'} : \mathcal{D}^t \rightarrow \mathbb{R}$ and real numbers β_l for $l = 1, \dots, r_g$ and $d = 1, \dots, d_{max}$. $\hat{f}(\mathbf{x}, \mathbf{d}, z) = \sum_{l=1}^{r_g} \phi_l(\mathbf{x}, z) \beta_l \prod_{d=1}^{d_{max}} \psi_{ld'}(m_{d'}(\mathbf{d}))$ such that*

$$\sup_{\mathbf{x} \in \bigcup_{t=2}^T \mathcal{X}^{1:t-1}, \mathbf{d} \in \bigcup_{t=1}^T \mathcal{D}^t, z \in \mathcal{Z}} \left| f(\mathbf{x}, \mathbf{d}, z) - \hat{f}(\mathbf{x}, \mathbf{d}, z) \right| \leq \epsilon. \quad (5)$$

Notes. Eq. (1) and Eq. (2) are motivated by the success of approaches for representation learning of sequences, which assumes that we can compile all the necessary information from the past using a current finite representation at any time step t . However, knowledge of Propositions 1 and 2 further imply that, for $f(n, d^{1:T}, x^{1:T}, z) := \mathbb{E}[X_n^t(d^{1:t}) | x_n(d^{1:t-1}), z_n]$, the representation of functions in a multilinear combination of adaptive factors (Eq. (1)) is motivated by more fundamental results in functional analysis. Our assumption that no value of d (other than the baseline 0) can be used more than once has mostly an empirical motivation, as this would imply unrealistic assumptions about the same intervention having the same effect when applied multiple times. Ultimately, we assume that the factors $h_{l_2}(d, t', t)$ leading to Eq. (2) are time-translation invariant, being a function of d and $t - t'$ only. While it is possible to generalize beyond translation invariant models, as commonly done in the synthetic controls literature [Abadie, 2021] that inspired the causal matrix factorization ideas [Athey et al., 2021, Agarwal et al., 2023b,c], this would complicate matters further by requiring a fourth factor into the summation term of Eq. (1) to encode absolute time. Models for time-series forecasting with parameter drifts can be tapped into and integrated with our model family, but we leave these out as future work.

Interpretation. At the starting of the process, where all units are assumed to be at their ‘‘natural’’ state (assuming $D_n^1 = 0$), we can interpret $\eta_n^1 := \beta_n$ as a finite basis representation, with respect to ϕ_n^1 , of $\mathbb{E}[X_n^1(0) | Z_n] = (\phi_n^1)^\top \eta_n^1$. Each η_n^1 can be seen as a latent feature of unit n . Effect vector ψ_n^t defines a *warping* of η_n^{t-1} that describes how treatments affect the behaviour of an individual with the resulting $\eta_n^t := \eta_n^{t-1} \odot \psi_n^t$. The modifier ψ_n^t can be interpreted as reverting, suppressing or promoting particular latent features that are assumed to encode all information necessary to reconstruct the conditional expectation of $X_n^t(d^{1:t})$ from the chosen basis (notice that intervention level 0 implies $\eta_n^t = \eta_n^{t-1}$ since we define $\psi_l(0, t', t) = 1$). This presents a sequential warping view of *compositionality* of interventions.

2.2 Identification and Data Assumptions

Assume for now that functions ϕ are known. As common in the literature of matrix factorization, assume also that we have access to some moments of the distribution. In particular, for given N data points and T time points, we have

access to $\mathbb{E}[X_n^t(d_n^{1:t}) \mid x_n^{t-1}(d_n^{1:t-1}), z_n]$. We will impose conditions on the realizations of $X_n^{1:T}$ and values chosen for $d_n^{1:T}$, as well as values of N and T as a function of r , in order to identify each β_n and the parameters of $\psi_l(d, t', t)$ for all intervention levels d of interest. The theoretical results presented, which describe how parameters are identifiable from *population* expectations and *known function spaces* determined by a prescribed basis ϕ of *known and finite dimensionality* r , will then provide a basis for a practical learning algorithm in the sequel.

Assumption 1 For a given individual n , we assume there is an initial period $T_{0n} \geq r$ with “no interventions” i.e., $D_n^t = 0$ for all $1 \leq t \leq T_{0n}$.

Assumption 2 let A_n be a $(T_{0n} - 1) \times r$ matrix where each row $t = 1, 2, \dots, T_{0n} - 1$ is given by $\phi_n(x_n^{1:t}(0^{1:t}), z_n)^\top$. We assume that A_n is full rank with left pseudo-inverse A_n^+ .

Proposition 3 Let b_n be a $(T_{0n} - 1) \times 1$ vector with entries $\mathbb{E}[X_n^{t+1}(d_n^{1:t+1}) \mid x_n^{1:t}(d_n^{1:t}), z_n]$. Under Assumptions 1 and 2, β_n is identifiable from A_n and b_n .

Assumption 3 For a given intervention level d , assume $\psi_l(d, t', t) \neq 0$ for all l, t, t' and that there is at least one time index t , and one set \mathcal{N}_d containing all units n where $d_n^{t+1} = d$, such that: (i) $N_d := |\mathcal{N}_d| \geq r$; (ii) $\forall n \in \mathcal{N}_d, d_n^{t+2} = \dots = d_n^{t+k_d-1} = 0$, where k_d is the dimensionality of the intervention level d .

Assumption 4 Let n_1, n_2, \dots, n_{N_d} index the elements of a set of units \mathcal{N}_d . For $t' = 1, 2, \dots, k_d - 1$, let $A_{dt'}$ be a $N_d \times r$ matrix where each row $i = 1, \dots, N_d$ is given by $\phi_{n_i}(x_{n_i}^{1:t+t'-1}(d_{n_i}^{1:t+t'-1}), z_{n_i})^\top$. We assume that each $A_{dt'}$ is full rank with left pseudo-inverse $A_{dt'}^+$.

This leads to the main result of this section:

Theorem 1 Assume we have a dataset of N units and T time points $(d_n^{1:T}, x_n^{1:T}, z_n)$ generated by a model partially specified by Eq. (1). Assume also knowledge of the conditional expectations $\mathbb{E}[X_n^t(d_n^{1:t}) \mid x_n^{t-1}(d_n^{1:t-1}), z_n]$ and basis functions $\phi_l(\cdot, \cdot)$ for all $l = 1, 2, \dots, r$ and all $1 \leq n \leq N$ and $1 \leq t \leq T$. Then, under Assumptions 1-4 applied to all individuals and all intervention levels d that appear in our dataset, we have that all β_n and all $\psi_l(d, \cdot, \cdot)$ are identifiable.

Notice that nothing above requires prior knowledge of all intervention levels which will exist, and could be applied on a rolling basis as new interventions are invented. There is no need for all units to start synchronously at $t = 1$: the framing of the theory assumes so to simplify presentation, but the only requirement is that each unit is given a “burn-in” period of at least T_0 steps and that each new intervention level d is applied to at least r units which have not been perturbed recently by relatively novel interventions (that is, units \mathcal{N}_d which, if they were given a past intervention not given to anyone else before, then that perturbation should have taken place enough steps in the past so that all recent but past ψ functions have been identified).

3 Algorithm and Statistical Inference

This section introduces a learning algorithm, and well as ways of quantifying uncertainties in prediction. We also allow for the learning of adaptive basis functions ϕ . As Eq. (1) does not define a generative model, which will be necessary for multiple-steps-ahead prediction, for the remainder of this section we will assume the likelihood implied by $X_n^t(d_n^{1:t}) = f(x_n^{1:t-1}(d_n^{1:t-1}), z_n) + \epsilon_n^t$. Here, the conditional mean $f(\cdot, \cdot)$ is given by Eq. (1) and $\epsilon_n^t \sim \mathcal{N}(0, \sigma^2)$, an error unaffected by D_n and other variables. Hence, σ^2 requires no further needs for identification results. In general, if our likelihood is defined via a finite set of estimating equations, we can parameterize it in the multilinear form analogous to (1) and repeat the analysis of the previous section. In practice, the functionals (such as the conditional expectations of X_t) used in an estimating equation are unknown. Matrix factorization methods can be applied directly by first performing a smoothing method on the data to get plug-in estimates of these functionals Squires et al. [2022], but we will adopt instead a likelihood-based approach.

3.1 Algorithm: CSI-VAE

We treat each β_n as a random effects vector, giving each entry β_{nl} an independent zero-mean Gaussian prior with variance σ_β^2 . Along with all hyperparameters, we optimize the (marginal) log-likelihood by gradient-based optimization. With a Gaussian likelihood, the posterior and filtering distribution of each β_n can be computed in closed form, but in our implementation we used a black-box amortised variational inference framework [Kingma and Welling, 2013, Mnih

and Gregor, 2014, Rezende et al., 2014] anyway that can be readily put together without specialized formulas and is easily adaptable to other likelihoods. We use a mean-field Gaussian approximation with posterior mean and variances produced by a gated recurrent unit (GRU) model [Chung et al., 2014] composed with a multilayer perceptron (MLP). The approximate posterior parameters at sample with t time steps are therefore $\mu_{q,\beta,n} := \text{MLP}(\text{GRU}_{\eta_{\beta,1}}(d_n^{1:t}, x_n^{1:t}, z_n))$, and $\log \sigma_{q,\beta,n} := \text{MLP}(\text{GRU}_{\eta_{\beta,2}}(d_n^{1:t}, x_n^{1:t}, z_n))$. Prediction for $X_n^{t+1:t+\Delta}$ is done by sampling M trajectories, where for each trajectory we first sample a new β_n from the mean-field Gaussian approximation. We set each forward \hat{X}_n^{t+i} to be the corresponding marginal Monte Carlo average. Each basis vector ϕ_n^t is parameterized via another GRU model such that $\phi_n^t := \text{MLP}(\text{GRU}_{\phi}(x_n^{1:t-1}, z_n))$. Although the theory in the previous section relies on known basis functions, we could train this GRU up to an threshold time point T_0 and freeze it from that point, each β_n being defined as the unit coefficient vector for this basis. In practice, we found that doing end-to-end learning provides a modest improvement, and this will be the preferred approach in the experiments. We do find that sometimes it is more stable to only use time series up to time point T_0 for the amortized β inference. Hence, we adopt this pipeline for any results reported in this paper, unless otherwise specified. We call our method *Compositional Sequential Intervention Variational Autoencoder (CSI-VAE)*.

3.2 Distribution-free Uncertainty Quantification

Conformal prediction (CP) Vovk et al. [2005], Fontana et al. [2023] provides prediction intervals with coverage guarantees. The intervals are computed using a calibration set of labeled samples and include the future samples with non-asymptotic lower-bounded probability. We consider Split Conformal Prediction in two setups.

1. **Hold-out predictions.** We have a set of *historical users*, $n = 1, \dots, N$, whose behaviour has been observed until time $t + \Delta$. The task is to predict the behaviour at time $t + \Delta$ of a *new user*, $n = N + 1$, who has been observed up to time t , i.e. to predict $X_{N+1}^{t+\Delta}$ given $X_{N+1}^{1:t}$ and $D_{N+1}^{1:t}$. If we assume we have used the history of the new user $X_n^{1:t}$, $n = 1, \dots, N + 1$, to train the model, calibration and test samples are exchangeable.
2. **Next-intervention predictions.** We have observed the behaviour of *all users*, $n = 1, \dots, N + 1$, up to time t and aim to predict the effects of the next intervention, which happens at time $t + 1$ for all users, i.e. $D_n^{t+1} \neq 0$, holding $D_n^{t+2:t+\Delta} = 0$. The task is to predict $X_n^{t+\Delta}(d_n^{1:t+\Delta})$ for $n = 1, \dots, N + 1$, but in what follows we will drop the potential outcome notation to keep notation lighter, referring to observed D . Calibration and test are *not exchangeable*, because i) the joint distribution after time t , $P_T \sim (X_n^{t+\Delta}, X_n^{1:t}, D_n^{1:t})$ may be different from the one before time t , $P_C \sim (X_n^{t'+\Delta}, X_n^{1:t'}, D_n^{1:t'})$, $t' < t - \Delta$ and ii) we only used $X_n^{t'}, D_n^{t'}$, $t' = 1, \dots, t$, for training.

CP algorithms are applied on top of given point-prediction models. In our case, the underlying model is f , which predicts the expected user behaviour at time $t + \Delta$ given the user history up to time t , i.e. $\hat{X}_n^{t+\Delta} := f(D_n^{1:t}, X_n^{1:t}, Z_n) \approx \mathbb{E}[X_n^{t+\Delta} | D_n^{1:t}, X_n^{1:t}, Z_n]$.

Setup 1. Calibration and test scores, $\{S_n = |X_n^{t+\Delta} - f(D_n^{1:t}, X_n^{1:t}, Z_n)|\}_{n=1}^N$ and $S_{N+1} = |X_{N+1}^{t+\Delta} - f(D_{N+1}^{1:t}, X_{N+1}^{1:t}, Z_n)|$ are exchangeable, i.e. $\text{Prob}(S_1, \dots, S_{N+1}) = \text{Prob}(S_{\sigma(1)}, \dots, S_{\sigma(N+1)})$ where σ is any permutation of $\{1, \dots, N + 1\}$. The Quantile Lemma, e.g. Lemma 1 of Tibshirani et al. [2019], implies the prediction interval

$$C = \{x \in \mathcal{X}, |x - \hat{X}_{N+1}^{t+\Delta}| \leq \hat{Q}_\alpha\} \quad (6)$$

$$\hat{Q}_\alpha = \inf_q \left\{ \sum_{n=1}^N \mathbf{1}(|X_n^{t+\Delta} - \hat{X}_n^{t+\Delta}| \leq q) \geq n_\alpha \right\}, \quad n_\alpha = \lceil (1 + N)(1 - \alpha) \rceil$$

is *valid* in the sense it obeys

$$\text{Prob}(X_{N+1}^{t+\Delta} \in C) \geq 1 - \alpha, \quad (7)$$

where the probability is over the calibration and test samples.

Setup 2. The prediction intervals defined in (6) may not be valid, i.e. (7) may not hold, because the calibration and test samples, $S_n^{t'} = |X_n^{t'+\Delta} - f(D_n^{1:t'}, X_n^{1:t'}, Z_n)|$ with $t' \leq t$ and $t' > t$, $n = 1, \dots, N$, are not exchangeable. Theorem 2 provides a bound on the coverage gap, i.e. a measure of violation of (7), under the assumption that the distribution shift is controlled by a perturbation parameter, $\epsilon > 0$.

Theorem 2 Assume we have N calibration samples,

$$S_n^{t'} = |X_n^{t'} - f(D_n^{1:t_n}, X_n^{1:t_n}, Z_n)|, \quad t' = t_n + \Delta < t, \quad n = 1, \dots, N \quad (8)$$

where t_n is the time user n experienced the last intervention before t . Assume there exists $\epsilon > 0$ such that, for all n ,

$$p_T(S_n^{t+\Delta}) = (1 - \epsilon)p_C(S_n^{t+\Delta}) + \epsilon p_\delta(S_n^{t+\Delta}), \quad (9)$$

where p_T and p_C are the (unknown) densities of the test and calibration distributions, p_δ is a bounded arbitrary shift density, and $p_{min} = \min_{n=1, \dots, N} p_C(S_n^{t'}) > 0$. Then,

$$\text{Prob}(X_{N+1}^{t+\Delta} \in C) \geq 1 - \alpha - \frac{1}{p_{min}} \frac{\epsilon}{1 - \epsilon}. \quad (10)$$

In the proof, we use the likelihood-ratio-weighting approach of Tibshirani et al. [2019] to obtain the empirical test distribution from the calibration samples and bound its quantile from below. The statement follows from standard inequalities on the mean and variance of the ϵ -perturbed distribution. We prefer this approach to conformal prediction adaptive models for time series, e.g. Gibbs and Candès [2021] or Angelopoulos et al. [2024], for two reasons: i) adaptive schemes have asymptotic coverage guarantees that can not be used to estimate the uncertainty on a single time step and ii) optimised density estimates are a byproduct of our prediction model.

4 Further Related Work

Brodersen et al. [2015] leverages Bayesian structural time-series models to estimate causal effects, and motivates our exponential decay model in Eq. (3). Unlike Brodersen et al. [2015], who focus on single interventions, our model explicitly addresses the complexity arising from sequential interventions, providing a more detailed perspective on the dynamic interplay of treatments over time. Several approaches for conformal prediction in causal inference have emerged in recent years [e.g., Tibshirani et al., 2019, Lei and Candès, 2021], including matrix completion Gui et al. [2023] and synthetic controls Chernozhukov et al. [2021]. Our focus has not been on individual nor average treatment effects, but directly on expected potential outcomes, similarly to the work on causal matrix completion Athey et al. [2021], Agarwal et al. [2023b,c], Squires et al. [2022]. Unlike the matrix completion literature, we focused on prediction problems, out-of-sample for both units and time steps. Moreover, the matrix completion literature is usually framed in terms of *marginal* expectations $\mathbb{E}[X_n^t(d)]$, as opposed to conditional expectations (notice that Agarwal et al. [2023c] considers covariates, but those are included as part of the generative model). Marginal models have some advantages when modeling multiple-step-ahead effects Evans and Didelez [2024], but they also involve complex computational considerations that we leave for future work. Finally, there is a rich literature on confounding adjustment where exogeneity of D_n^t cannot be assumed, see Hernán and J [2020] for a textbook treatment. Some of the causal matrix completion literature takes the perspective that factors such as β_n could be interpreted as latent factors conditional on which ignorability could be assumed. However, we consider this assumption hard to justify due to the unknown nature of β_n . We can rely on standard approaches of sequential ignorability Robins [1997] to justify our method in the absence of randomization.

5 Experiments

We run a number of synthetic and semi-synthetic experiments to evaluate the performance of the CSI-VAE approach. In this section, we summarize our experimental set-up and main results. The code for reproducing all results and figures is available online²; in Appendix C, we provide a detailed description of the datasets and models; in Appendix D, we present further analysis and more results; and in Appendix E we present a demo for uncertainty quantification results.

Datasets and oracular simulators. The first step to assess intervention predictions is to build a set of proper ground truth test beds, where we can control different levels of combinations of interventions. We build two sets of oracular simulators. (1) The **Fully-synthetic** simulator is constructed primarily based on random models following our parameterization in Section 2. (2) The **Semi-synthetic** simulator is constructed based on a real-world dataset from Spotify³ which aims to predict skip behaviour of users based on its past interaction history. See details in Appendix C. For each type of simulator, we generate 5 different versions with different random seeds. From simulator (1), we construct a simulated datasets of size 50,000, containing 5 different interventions happening to the units at any time

²The code will be released upon acceptance, and is available in the supplementary material.

³<https://open.spotify.com/>

Table 1: Main experimental results, averaged mean squared root error over five different seeds.

Model	Full Synthetic					Semi-Synthetic Spotify				
	T+1	T+2	T+3	T+4	T+5	T+1	T+2	T+3	T+4	T+5
CSI-VAE-1	36.53	41.46	41.73	41.12	41.32	68.23	82.94	83.53	81.97	79.63
CSI-VAE-2	97.80	118.25	117.79	127.25	135.03	253.85	312.53	305.08	303.68	302.83
CSI-VAE-3	138.78	164.02	141.71	132.59	125.55	757.94	937.07	800.55	704.66	634.72
GRU-0	229.72	269.66	220.95	208.30	188.43	215.42	260.65	193.41	137.20	117.06
GRU-1	230.76	270.83	220.93	208.33	184.92	223.61	269.69	205.91	141.53	126.36
GRU-2	93.73	101.03	118.01	88.53	132.28	154.18	187.42	177.96	133.36	127.58

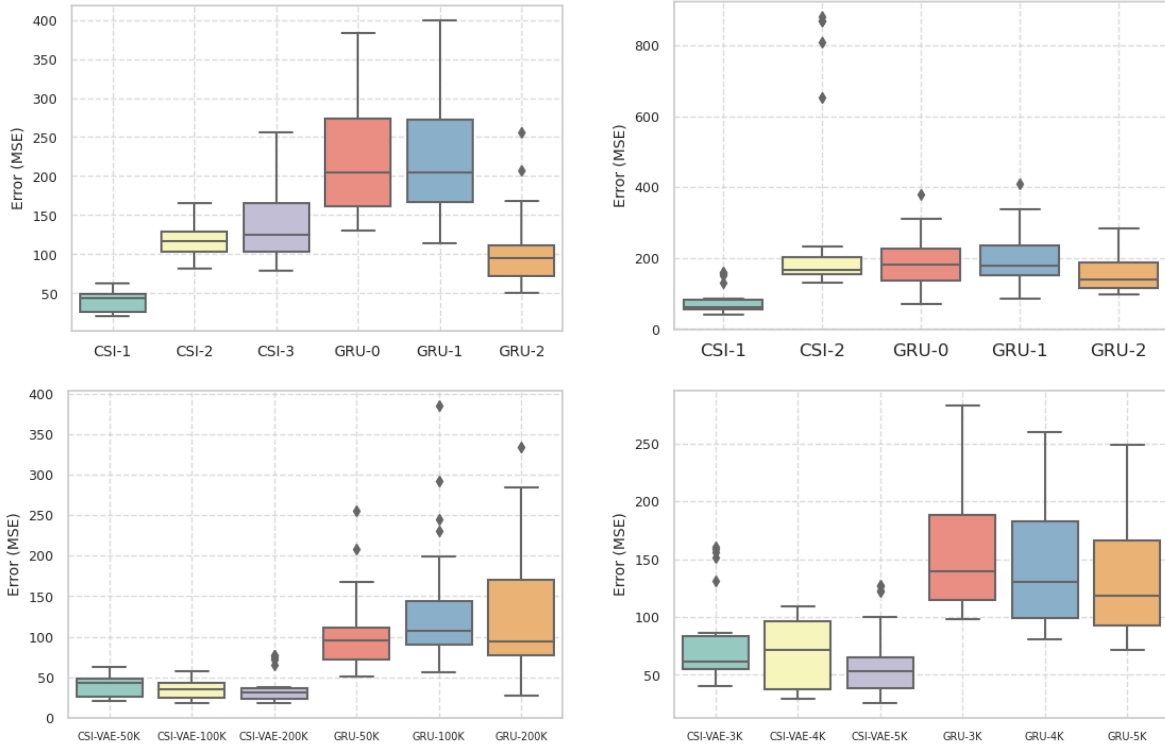


Figure 2: **Top**: 5-run evaluation of test mean squared error on the fully-synthetic (left) and semi-synthetic cases (case). CSI-3 was removed on the right due to very high errors. **Bottom**: how errors change as training sizes are increased, CSI-1 vs. GRU-2 (left: fully-synthetic, right: semi-synthetic).

after an initial burn-in period of $T_0 = 10$, although only maximum 3 of these can be observed for any given unit, with $r = 5$ being the true dimensions of the model. For simulator (2), we construct simulated datasets of size 3,000, again containing 5 different interventions, an initial period $T_0 = 25$, a maximum 3 different interventions per unit and $r = 10$. For making predictions, we predict outcomes for interventions not applied yet within any given unit (i.e. at least from the 2 options left). In simulator (2) parameters ϕ and β are learned from real-world data. Interventions are artificial, but inspired by the process of showing different proportions of track types to an user in a Spotify-like environment. For both setups, we use a data ratio of 0.7, 0.1, 0.2 for training, validation and test, respectively. We report the final results in Table 1 with another constructed holdout set (5,000 for fully-synthetic and 1,000 for semi-synthetic).

Compared models. We implemented three variations: (1) **CSI-VAE-1** follows exactly our setup in Section 2; (2) **CSI-VAE-2** can be considered as an ablation study, which relaxes the product form of Eq. 1 and replace it with a black-box MLP applied directly to $(\phi_n^t, \beta_n, \psi_n^t)$ (and hence may not guarantee identifiability); (3) **CSI-VAE-3** as another ablation study, where the equation for ψ (Eq. (2)) is replaced by a black-box function taking the sequence of interventions D as a standard time series. We compare our model against: (1) **GRU-0**, a black-box gated recurrent unit (GRU, Cho et al. [2014]) composed with a MLP, using only the past history of $X_n^{1:t}$ and Z_n ; (2) **GRU-1**, another GRU

Table 2: P-values from two-sample t-tests against the null hypothesis that models perform no better on average than its counterpart. Significance at 0.05 indicated with one asterisk, 0.001 with two.

Model	Full Synthetic					Semi-Synthetic Spotify				
	CSI-VAE-2	CSI-VAE-3	GRU-0	GRU-1	GRU-2	CSI-VAE-2	CSI-VAE-3	GRU-0	GRU-1	GRU-2
CSI-VAE-1	< 0.001**	< 0.001**	< 0.001**	< 0.001**	< 0.001**	< 0.001**	< 0.001**	< 0.001**	< 0.001**	< 0.001**
CSI-VAE-2	\	0.057	< 0.001**	< 0.001**	0.249	\	< 0.001**	0.058	0.081	< 0.05*
CSI-VAE-3	\	\	< 0.001**	< 0.001**	< 0.05*	\	\	< 0.001**	< 0.001**	< 0.001**
GRU-0	\	\	\	0.990	< 0.001**	\	\	\	0.705	0.129
GRU-1	\	\	\	\	< 0.001**	\	\	\	\	0.061

composed with a MLP that takes into account also the latest intervention D_n^t ; and (3) **GRU-2**, which uses not only D_n^t but also the entire past history $D_n^{1:t}$ just like CSI-VAE. In general, GRU-2 can be considered as a very strong and generic black-box baseline model.

Results. Each experiment was repeated 5 times, using Adam Kingma and Ba [2015] at a learning rate of 0.01, with 50 epochs in the fully-synthetic case and 100 for the semi-synthetic, which was enough for convergence. We selected the best iteration point based on small holdout set. The main results are presented in Tables 1 and 2, which shows the superiority of our model against the strong baselines. We also observed that the identifiable results and compositional interactions of intervention effect are both critical, as evidenced by the drop in performance for CSI-VAE 2 and 3 in Table 1. In Appendix D, we provide the following further experiments: (1) different choices of r (to summarize: using r less than the true value gracefully underfits, while there is evidence of small overfitting for choices of r which overshoot the true value but where we can enforce regularization techniques); (2) different size of the training data (to summarize: even with more data provided, our model consistently outperforms the blackbox models by a significant margin. We show that a generic blackbox cannot solve this problem by simply feeding in more data); and (3) a demonstration of conformal prediction that allow us to better calibrate the predictive coverage compared to vanilla model-based prediction.

6 Conclusion

We introduced an approach for predicting potential outcomes with a careful accounting of when extrapolation to unseen sequences are warranted. **Lessons.** Embeddings are important given sparse categorical sequential data see e.g. [Vaswani et al., 2017]. However, large combinatorial interventional spaces benefit from models that more carefully lay down conditions for identification. **Limitations.** Unlike the traditional synthetic control literature Abadie [2021], we assume a model for time effects based on autoregression and truncated or parametric temporal-intervention interactions. While it is possible to empirically evaluate the prediction abilities of the model using a validation sample, high-stakes applications (such as major interventions to counteract the effect of a pandemic) should take into consideration that uncontrolled distribution shifts may take place, and careful modeling of such shifts should be added to any analytical pipeline to avoid damaging societal implications. **Future Work.** Besides allowing for an explicit parameterization of drifts, an explicit account for modeling when unmeasured confounding may have been presented in the selection of past interventions is necessary to increase the applicability of the method to more sources of data.

Acknowledgements

We thank Zhenwen Dai and Georges Dupret for many helpful comments and suggestions. JY and RS were partially funded by the EPSRC Open Fellowship EP/W024330/1. RS acknowledges further funding from the EPSRC AI Hub for Causality in Healthcare AI with Real Data, EP/Y028856/1.

References

- A. Abadie. Using synthetic controls: Feasibility, data requirements, and methodological aspects. *Journal of Economic Literature*, 59:391–425, 2021.
- A. Agarwal, A. Agarwal, and S. Vijaykumar. Synthetic combinations: A causal inference framework for combinatorial interventions. *Advances in Neural Information Processing Systems 36 (NeurIPS 2023)*, pages 19195–19216, 2023a.
- A. Agarwal, M. Dahleh, D. Shah, and D. Shen. Causal matrix completion. *Proceedings of Thirty Sixth Conference on Learning Theory*, pages 3821–3826, 2023b.
- A. Agarwal, D. Shah, and D. Shen. Synthetic interventions. *arXiv:2006.07691 (econ)*, 2023c.

- V. Aglietti, X. Lu, A. Paleyes, and J. Gonz'alez. Causal Bayesian optimization. *Proceedings of the Twenty Third International Conference on Artificial Intelligence and Statistics*, 34:3155–3164, 2020.
- Anastasios Angelopoulos, Emmanuel Candes, and Ryan J Tibshirani. Conformal pid control for time series prediction. *Advances in Neural Information Processing Systems*, 36, 2024.
- S. Athey, M. Bayati, N. Doudchenko, G. Imbens, and K. Khosravi. Matrix completion methods for causal panel data models. *Journal of the American Statistical Association*, 116:1716–1730, 2021.
- G. Bravo-Hermesdorff, D. Watson, J. Yu, J. Zeitler, and R. Silva. Intervention generalization: A view from factor graph models. *Advances in Neural Information Processing Systems 36 (NeurIPS 2023)*, pages 43662–43675, 2023.
- K. Brodersen, F. Gallusser, J. Koehler, N. Remy, and S. Scott. Inferring causal impact using Bayesian structural time-series models. *Annals of Applied Statistics*, to appear, 2015.
- Brian Brost, Rishabh Mehrotra, and Tristan Jehan. The music streaming sessions dataset. In *The World Wide Web Conference*, pages 2594–2600, 2019.
- B. Chakraborty and E. Moodie. *Statistical Methods for Dynamic Treatment Regimes: Reinforcement Learning, Causal Inference, and Personalized Medicine*. Springer, 2013.
- Victor Chernozhukov, Kaspar Wuthrich, and Yinchu Zhu. An exact and robust conformal inference method for counterfactual and synthetic controls. *Journal Of The American Statistical Association*, 116(536):1849–1864, OCT 2 2021. ISSN 0162-1459. doi: 10.1080/01621459.2021.1920957.
- K. Cho, B. van Merriënboer, C. Gulcehre, D. Bahdanau, F. Bougares, H. Schwenk, and Y. Bengio. Learning phrase representations using RNN encoder–decoder for statistical machine translation. *Proceedings of the 2014 Conference on Empirical Methods in Natural Language Processing (EMNLP 2014)*, pages 1724–1734, 2014.
- Junyoung Chung, Caglar Gulcehre, KyungHyun Cho, and Yoshua Bengio. Empirical evaluation of gated recurrent neural networks on sequence modeling. *arXiv preprint arXiv:1412.3555*, 2014.
- J. Correa and E. Bareinboim. A calculus for stochastic interventions: causal effect identification and surrogate experiments. *Proceedings of the AAAI Conference on Artificial Intelligence (AAAI 2020)*, 34:10093–10100, 2020.
- P. Dawid. Decision-theoretic foundations for statistical causality. *Journal of Causal Inference*, 9(56):39–77, 2021.
- V. Didelez, A. P. Dawid, and S. Geneletti. Direct and indirect effects of sequential treatments. *Proceedings of the Twenty-Second Conference on Uncertainty in Artificial Intelligence (UAI2006)*, 2006.
- R. Evans and V. Didelez. Parameterizing and simulating from causal models. *Journal of the Royal Statistical Society. Series B (Statistical Methodology)*, 2024. URL <https://doi.org/10.1093/jrsssb/qkad058>.
- Matteo Fontana, Gianluca Zeni, and Simone Vantini. Conformal prediction: A unified review of theory and new challenges. *Bernoulli*, 29(1):1–23, FEB 2023. ISSN 1350-7265. doi: 10.3150/21-BEJ1447.
- Isaac Gibbs and Emmanuel Candes. Adaptive conformal inference under distribution shift. *Advances in Neural Information Processing Systems*, 34:1660–1672, 2021.
- Y. Gui, R. Barber, and C. Ma. Conformalized matrix completion. *Advances in Neural Information Processing Systems*, 36:4820–4844, 2023.
- M. Hernán and Robins J. *Causal Inference: What If*. Chapman & Hall/CRC, 2020.
- S. Hochreiter and J. Schmidhuber. Long short-term memory. *Neural Computation*, 9:1735–1780, 1997.
- G. W. Imbens and D. B. Rubin. *Causal Inference in Statistics, Social, and Biomedical Sciences: An Introduction*. Cambridge University Press, 2015.
- J. Kaddour, Y. Zhu, Q. Liu, M. J. Kusner, and R. Silva. Causal effect inference for structured treatments. *Advances in Neural Information Processing Systems 34 (NeurIPS 2021)*, pages 24841–24854, 2021.
- D. Kingma and J. Ba. Adam: A method for stochastic optimization. *3rd International Conference for Learning Representations*, 2015.
- Diederik P Kingma and Max Welling. Auto-encoding variational bayes. *arXiv preprint arXiv:1312.6114*, 2013.
- L. Lei and E. J. Candès. Conformal inference of counterfactuals and individual treatment effects. *Journal of the Royal Statistical Society Series B: Statistical Methodology*, 83(5):911–938, 2021.
- Andriy Mnih and Karol Gregor. Neural variational inference and learning in belief networks. In *International Conference on Machine Learning*, pages 1791–1799. PMLR, 2014.
- S. Murphy. Optimal dynamic treatment regimes. *Journal of the Royal Statistical Society Series B*, 6(2):331–355, 2003.

- R. Nabi, T. McNutt, and I. Shpitser. Semiparametric causal sufficient dimension reduction of multidimensional treatments. *The 38th Conference on Uncertainty in Artificial Intelligence*, pages 1445–1455, 2022.
- J. Pearl. *Causality: Models, Reasoning and Inference, 2nd edition*. Cambridge University Press, 2009.
- Danilo Jimenez Rezende, Shakir Mohamed, and Daan Wierstra. Stochastic backpropagation and approximate inference in deep generative models. In *International conference on machine learning*, pages 1278–1286. PMLR, 2014.
- James Robins. A new approach to causal inference in mortality studies with a sustained exposure period—application to control of the healthy worker survivor effect. *Mathematical modelling*, 7(9-12):1393–1512, 1986.
- James M Robins. Causal inference from complex longitudinal data. In *Latent variable modeling and applications to causality*, pages 69–117. Springer, 1997.
- S. Saengkyongam, Rosenfeld, P. Ravikumar, N. Pfister, and J. Peters. Identifying representations for intervention extrapolation. *International Conference on Learning Representations (ICLR 2024)*, 2024.
- Y. Saito, R. Qingyang, and T. Joachims. Off-policy evaluation for large action spaces via conjunct effect modeling. *Proceedings of the 39th International Conference on Machine Learning (ICML 2023)*, pages 29734—29759, 2023.
- Y. Saito, J. Yao, and T. Joachims. POTEC: Off-policy learning for large action spaces via two-stage policy decomposition. *Proceeding of the 40th International Conference on Machine Learning (ICML 2024)*, 2024.
- A.M. Schäfer and H.-G. Zimmermann. Recurrent neural networks are universal approximators. *International Journal of Neural Systems*, 17(04):253–263, 2007.
- P. Spirtes, C. Glymour, and R. Scheines. *Causation, Prediction and Search*. Cambridge University Press, 2000.
- C. Squires, D. Shen, A. Agarwal, D. Shah, and C. Uhler. Causal imputation via synthetic interventions. *First Conference on Causal Learning and Reasoning (CLear 2021)*, pages 688–711, 2022.
- R. Sutton and A. Barto. *Reinforcement Learning: An Introduction*. MIT Prsss, 2018.
- Ryan J Tibshirani, Rina Foygel Barber, Emmanuel Candes, and Aaditya Ramdas. Conformal prediction under covariate shift. *Advances in neural information processing systems*, 32, 2019.
- A. Vaswani, N. Shazeer, N. Parmar, J. Uszkoreit, L. Jones, A. Gomez, Ł. Kaiser, and I. Polosukhin. Attention is all you need. *Advances in Neural Information Processing Systems 31 (NIPS 2017)*, pages 6000–6010, 2017.
- V. Vovk, A. Gammernan, and G. Shafer. *Algorithmic Learning in a Random World*. Springer, 2005.
- L. Yao, S. Li, Y. Li, H. Xue, J. Gao, and A. Zhang. On the estimation of treatment effect with text covariates. *Proceedings of the Twenty-Eighth International Joint Conference on Artificial Intelligence (IJCAI-19)*, pages 4106–4113, 2019.
- Z. Zeng, S. Balakrishnan, Y. Han, and E. Kennedy. Causal inference with high-dimensional discrete covariates. *arXiv:2405.00118 (math)*, 2024.
- J. Zhang and E. Bareinboim. Designing optimal dynamic treatment regimes: A causal reinforcement learning approach. *Proceedings of the 37th International Conference on Machine Learning (ICML 2020)*, 2020.
- J. Zhang, K. Greenewald, C. Squires, A. Srivastava, K. Shanmugam, and C. Uhler. Identifiability guarantees for causal disentanglement from soft interventions. *Advances in Neural Information Processing Systems*, 36:50254–50292, 2023.

Appendix

A General Background

Much of traditional causal inference aimed at estimating an outcome of a fixed treatment that does not vary over time Imbens and Rubin [2015]. However, many causal questions involves treatments that vary over time. For example, we might be interested in estimating the causal effects of medical treatments, lifestyle habits, employment status, marital status, occupation exposures, etc. Because these treatments may take different values for a single individual over time, hence they are often refereed to as time-varying treatments [Hernán and J, 2020].

In many designs, it is assumed that a time-fixed treatment applied to individuals in our population happens at the same time (i.e. there is a shared global clock for everyone). A more relaxed setting (and more practical, as described in this paper) is that (categorical) interventions can happen to different individuals at different time steps, potentially resulting in no two identically distributed time-series. The purpose now is to estimate the causal effect or predict expected outcomes under time-varying treatments as a time-series, rather than estimating missing potential outcome snapshots at fixed time interval that has passed already.

One typical way of designing experiments under a binary treatment (0 or 1) [Robins, 1986, 1997] of time-varying treatments is to have $\bar{d}_0 = (0, 0, \dots, 0)$ (never treated) and $\bar{d}_1 = (1, 1, \dots, 1)$ (always treated) as the two options in the design space. This allows us to answer what the average expected outcome contrasted between these two options. A fine-grained estimation at every time step will require further levels of contrast under two regimes, such as $d = (0, 1, \dots, 1)$ and $d = (1, 0, \dots, 0)$. However, the number of combinations grows exponentially on T , the number of time steps, even when only binary treatments are at the stake. In this paper, we focus on static treatment strategies where the treatment is randomly assigned (also referred to as a sequential randomized experiment), although the next intervention in a sequential randomised experiment can depend on previous step intervention, as long as there is no influence from unobserved confounders.

Conditional ignorability holds when we are able to block unmeasured confounders using observable confounders only. Similarly, in a time-varying setting, we achieve sequential conditional ignorability by conditioning on the time-varying covariates, including past actions (Hernán and J [2020], and Chapter 4 of Pearl [2009]). In our manuscript, we will have little to say about the uses of conditional sequential ignorability and other adjustment techniques for observational studies, as these ideas are well-understood and can be applied on top of our main results. Hence, we decided to focus on treatments that act as-if randomized so that we can explore in more detail our contributions.

B Proofs

Proposition 1 *Let $f(n, d^{1:T}, x^{1:T}, z) := f_d^\top(d^{1:T})f_{nxz}(n, x^{1:T}, z)$, where function sequences $f_d(d^{1:T})$ and $f_{nxz}(n, x^{1:T}, z)$ are defined for all $T \in \mathbb{N}^+$ and have codomain \mathbb{R}^{r_s} . Furthermore, define $f_{dl}(d^{1:T})$ as in Eq. (4) with $r_h = 1$, and the l -th entry of $f_{nxz}(n, x^{1:T}, z)$ as $f_{nxzl}(n, x^{1:T}, z) := u_l(n)^\top v_l(x^{1:T}, z)$, each of the latter having codomain $\mathbb{R}^{r_{s'}}$ and where $v_l(\cdot, \cdot)$ is defined recursively for any T , similarly $g_l(\cdot, \cdot, \cdot)$. Then there exists some integer r and three functions a, b and c with codomain \mathbb{R}^r so that $f(n, d^{1:T}, x^{1:T}, z) = \sum_{l=1}^r a_l(n) \times b_l(x^{1:T}, z) \times c_l(d^{1:T}, T)$. Moreover $c_l(d^{1:T}, T) = \prod_{t=1}^T m_l(d^t, t, T)$ for functions $m_l : \mathbb{N}^3 \rightarrow \mathbb{R}$.*

Proof. The proof is tedious and the result intuitive, but they help to formalize the main motivation for Eqs. (1) and (3).

$$\begin{aligned} f_d^\top(d^{1:T})f_{nxz}(n, x^{1:T}, z) &= \sum_{l'=1}^{r_s} f_{dl'}(d^{1:T})f_{nxzl'}(n, x^{1:T}, z) \\ &= \sum_{l'=1}^{r_s} f_{dl'}(d^{1:T}) \sum_{l''=1}^{r_{s'}} u_{l'l''}(n) v_{l'l''}(x^{1:T}, z) \\ &= \sum_{l'=1}^{r_s} \sum_{l''=1}^{r_{s'}} u_{l'l''}(n) v_{l'l''}(x^{1:T}, z) f_{dl'}(d^{1:T}) \\ &= \sum_{l=1}^r a_l(n) b_l(x^{1:T}, z) c_l(d^{1:T}), \end{aligned}$$

where $r = r_s \times r_{s'}$ and $a_l(n) := u_{l'l''}(n)$ for $l = l' \times l''$; $b_l(x^{1:T}, z) := v_{l'l''}(x^{1:T}, z)$ for $l = l' \times l''$; and $c_l(d^{1:T}) = f_{dl'}(d^{1:T})$ for $l' = \lceil l/r_{s'} \rceil$, where $\lceil \cdot \rceil$ is the ceiling function.

Finally, each $c_l(d^{1:T})$ is by definition some $f_{dl'}(d^{1:T})$. From Eq. (4) and the assumptions, $f_{dl'}(d^{1:T}) = g_{l'}(d^{1:T}, T, T)$, and $g_{l'}(d^{1:t}, t', t) := h_{l'}(g_l(d^{1:t'-1}, t' - 1, t), d^{t'}, t', t)$ for $t' > 0$ and $d > 0$, with otherwise $h_{l'_1}(g_{l'}(d^{1:t}, t' - 1, t))h_{l'_2}(d^t, t', t)$. For $t' = 0$, $h_{l'}(v, d, t', t) \equiv 1$, and for $t' > 0$ and $d = 0$, $h_{l'}(v, d, t', t) \equiv g_{l'}(d^{1:t'-1}, t' - 1, t)$. By recursive application, this implies $f_{dl'}(d^{1:T}) = \prod_{t'=1: d^{t'} > 0}^T h_{l'_2}(d^{t'}, t', T)$ and the result follows. \square

Proposition 2 Suppose we have a measurable function $f : \bigcup_{t=2}^T \mathcal{X}^{1:t-1} \times \bigcup_{t=1}^T \mathcal{D}^t \times \mathcal{Z} \rightarrow \mathbb{R}^d$, $t \leq T$, where $\mathcal{X}^{1:t-1}$ and \mathcal{Z} are compact, \mathcal{D}^t is finite. For $d = 1, \dots, d_{max}$, let $m_d : \bigcup_{t=1}^T \mathcal{D}^t \rightarrow \{1, \dots, t\}$ with $m_d(\mathbf{d}) = t$ if $\exists t$ s.t. $\mathbf{d}_t = d$ else 0. There exist $L = O(T^{d_{max}+1})$ such that for any ϵ , there are measurable functions $\phi_l : \mathcal{X}^{1:t-1} \times \mathcal{Z} \rightarrow \mathbb{R}^d$ and $\psi_{ld'} : \mathcal{D}^t \rightarrow \mathbb{R}$ and real numbers β_l for $l = 1, \dots, r$ and $d = 1, \dots, d_{max}$, $\hat{f}(\mathbf{x}, \mathbf{d}, z) = \sum_{l=1}^L \phi_l(\mathbf{x}, z) \beta_l \prod_{d=1}^{d_{max}} \psi_{ld'}(m_{d'}(\mathbf{d}))$ such that

$$\sup_{\mathbf{x} \in \bigcup_{t=2}^T \mathcal{X}^{1:t-1}, \mathbf{d} \in \bigcup_{t=1}^T \mathcal{D}^t, z \in \mathcal{Z}} |f(\mathbf{x}, \mathbf{d}, z) - \hat{f}(\mathbf{x}, \mathbf{d}, z)| \leq \epsilon \quad (11)$$

Proof. First note that we can construct an equivalent definition of \mathcal{D}^t for some fixed t as follows. We for now call the new object $\bar{\mathcal{D}}^t$.

$$\bar{\mathcal{D}}^t = \left\{ \mathbf{v} \in \mathbb{R}^{d_{max}} \mid v_d \in \{0, \dots, t\} \forall d; v_{d'} \neq v_d \text{ whenever } d' \neq d \text{ and } v_d \neq 0 \right\} \quad (12)$$

Note that there is a one-to-one correspondence between $\bar{\mathcal{D}}^t$ and \mathcal{D}^t , and denote the bijection connecting them by $g : \bar{\mathcal{D}}^t \rightarrow \mathcal{D}^t$. Since both sets are finite, we can approximate f with \hat{f} , if and only if we can approximate $f \circ i \times g \times i$ by $\hat{f} \circ i \times g \times i$. So wlog just consider $\bar{\mathcal{D}}^t$ as \mathcal{D}^t .

The set of all sequences of treatments is the union of \mathcal{D}^t over $t = 1, \dots, T$, for some known T :

$$\mathcal{D}^{\mathcal{T}} = \bigcup_{t=1}^T \mathcal{D}^t \text{ known } T. \quad (13)$$

Note that

$$|\mathcal{D}^t| < (t+1)^{d_{max}} \quad (14)$$

$$|\mathcal{D}^{\mathcal{T}}| < \sum_{t=1}^T (t+1)^{d_{max}} \quad (15)$$

therefore the size of $\mathcal{D}^{\mathcal{T}}$ is polynomial in T .

Now note, fixing the ground truth function f at $D \in \mathcal{D}^{\mathcal{T}}$ gives me a new function $\bigcup_{t=1}^T \mathcal{X}^{\infty: \lfloor -\infty} \times \mathcal{Z} \rightarrow \mathcal{X}$. Analogously, fixing \hat{f} at some $D \in \mathcal{D}^{\mathcal{T}}$ also give a new function in the same function space. Since $\mathcal{D}^{\mathcal{T}}$ is finite, we can enumerate its elements. Thus for every $D^{(i)} \in \mathcal{D}^{\mathcal{T}}$, $i = 1, \dots, |\mathcal{D}^{\mathcal{T}}|$, write down \hat{f} fixed at $D^{(i)}$:

$$\hat{f}(X^{1:t-1}, D^{(i)}, Z) = \sum_{l=1}^r \phi_l(X^{1:t-1}, Z) \beta_l \psi_{l1}(D_1^{(i)}) \psi_{l2}(D_2^{(i)}) \cdots \psi_{ld_{max}}(D_{d_{max}}^{(i)}) \quad (16)$$

Then we can express the vector field:

$$\begin{pmatrix} \hat{f}(\cdot, D^{(1)}, \cdot) \\ \vdots \\ \hat{f}(\cdot, D^{(|\mathcal{D}^{\mathcal{T}}|)}, \cdot) \end{pmatrix} = \underbrace{\begin{pmatrix} \beta_1 \prod_{d=1}^{d_{max}} \psi_{1d}(D_1^{(1)}) & \cdots & \beta_r \prod_{d=1}^{d_{max}} \psi_{rd}(D_1^{(1)}) \\ \vdots & \vdots & \vdots \\ \beta_1 \prod_{d=1}^{d_{max}} \psi_{1d}(D_1^{(|\mathcal{D}^{\mathcal{T}}|)}) & \cdots & \beta_r \prod_{d=1}^{d_{max}} \psi_{rd}(D_1^{(|\mathcal{D}^{\mathcal{T}}|)}) \end{pmatrix}}_W \begin{pmatrix} \phi_1(\cdot, \cdot) \\ \vdots \\ \phi_r(\cdot, \cdot) \end{pmatrix} \quad (17)$$

By choosing $r = |\mathcal{D}^{\mathcal{T}}|$ and appropriate values for β_l and $\psi_{ld}(D^{(i)})$, we can make W invertible.

Now consider the vector field given by the ground truth function fixed at all values of $D \in \mathcal{D}^{\mathcal{T}}$:

$$\begin{pmatrix} f(\cdot, D^{(1)}, \cdot) \\ \vdots \\ f(\cdot, D^{(|\mathcal{D}^{\mathcal{T}}|)}, \cdot) \end{pmatrix} \quad (18)$$

And consider its transformation under W^{-1} :

$$W^{-1} \begin{pmatrix} f(\cdot, D^{(1)}, \cdot) \\ \vdots \\ f(\cdot, D^{(|\mathcal{D}^{\mathcal{T}}|)}, \cdot) \end{pmatrix} \quad (19)$$

Since recurrent neural networks are universal approximators Schäfer and Zimmermann [2007], for every $\delta > 0$ we can choose ϕ_1, \dots, ϕ_r so that

$$\sup_{\mathbf{x} \in \bigcup_{t=2}^T \mathcal{X}^{1:t-1}, z \in \mathcal{Z}} \left\| \begin{pmatrix} \phi_1(\mathbf{x}, z) \\ \vdots \\ \phi_r(\mathbf{x}, z) \end{pmatrix} - W^{-1} \begin{pmatrix} f(\mathbf{x}, D^{(1)}, z) \\ \vdots \\ f(\mathbf{x}, D^{(|\mathcal{D}^T|)}, z) \end{pmatrix} \right\|_2 \leq \delta \quad (20)$$

Since W is a finite matrix, its operator norm is well-defined. Then

$$\sup_{\mathbf{x} \in \bigcup_{t=2}^T \mathcal{X}^{1:t-1}, z \in \mathcal{Z}} \left\| W \begin{pmatrix} \phi_1(\mathbf{x}, z) \\ \vdots \\ \phi_r(\mathbf{x}, z) \end{pmatrix} - \begin{pmatrix} f(\mathbf{x}, D^{(1)}, z) \\ \vdots \\ f(\mathbf{x}, D^{(|\mathcal{D}^T|)}, z) \end{pmatrix} \right\|_2 \quad (21)$$

$$\leq \sup_{\mathbf{x} \in \bigcup_{t=2}^T \mathcal{X}^{1:t-1}, z \in \mathcal{Z}} \|W\|_{op}^2 \left\| \begin{pmatrix} \phi_1(\mathbf{x}, z) \\ \vdots \\ \phi_r(\mathbf{x}, z) \end{pmatrix} - W^{-1} \begin{pmatrix} f(\mathbf{x}, D^{(1)}, z) \\ \vdots \\ f(\mathbf{x}, D^{(|\mathcal{D}^T|)}, z) \end{pmatrix} \right\|_2^2 \quad (22)$$

$$\leq \|W\|_{op}^2 \sup_{\mathbf{x} \in \bigcup_{t=2}^T \mathcal{X}^{1:t-1}, z \in \mathcal{Z}} \left\| \begin{pmatrix} \phi_1(\mathbf{x}, z) \\ \vdots \\ \phi_r(\mathbf{x}, z) \end{pmatrix} - W^{-1} \begin{pmatrix} f(\mathbf{x}, D^{(1)}, z) \\ \vdots \\ f(\mathbf{x}, D^{(|\mathcal{D}^T|)}, z) \end{pmatrix} \right\|_2 \quad (23)$$

$$\leq \|W\|_{op}^2 \delta \quad (24)$$

But

$$\sup_{\mathbf{x} \in \bigcup_{t=2}^T \mathcal{X}^{1:t-1}, \mathbf{d} \in \mathcal{D}^T, z \in \mathcal{Z}} |f(\mathbf{x}, \mathbf{d}, z) - \hat{f}(\mathbf{x}, \mathbf{d}, z)| \quad (25)$$

$$= \left(\sup_{\mathbf{x} \in \bigcup_{t=2}^T \mathcal{X}^{1:t-1}, z \in \mathcal{Z}} \max_{\mathbf{d} \in \mathcal{D}^T} |f(\mathbf{x}, \mathbf{d}, z) - \hat{f}(\mathbf{x}, \mathbf{d}, z)|^2 \right)^{1/2} \quad (26)$$

$$\leq \left(\sup_{\mathbf{x} \in \bigcup_{t=2}^T \mathcal{X}^{1:t-1}, z \in \mathcal{Z}} \sum_{\mathbf{d} \in \mathcal{D}^T} |f(\mathbf{x}, \mathbf{d}, z) - \hat{f}(\mathbf{x}, \mathbf{d}, z)|^2 \right)^{1/2} \quad (27)$$

$$= \left(\sup_{\mathbf{x} \in \bigcup_{t=2}^T \mathcal{X}^{1:t-1}, z \in \mathcal{Z}} \left\| W \begin{pmatrix} \phi_1(\mathbf{x}, z) \\ \vdots \\ \phi_r(\mathbf{x}, z) \end{pmatrix} - \begin{pmatrix} f(\mathbf{x}, D^{(1)}, z) \\ \vdots \\ f(\mathbf{x}, D^{(|\mathcal{D}^T|)}, z) \end{pmatrix} \right\|_2^2 \right)^{1/2} \quad (28)$$

$$\leq \|W\|_{op}^2 \delta \quad (29)$$

So choosing $\delta = \epsilon / \|W\|_{op}^2$ would give us the desired result.

□

Proposition 3 Let b_n be a $(T_{0_n} - 1) \times 1$ vector, where each entry t is given by $\mathbb{E}[X_n^{t+1}(d_n^{1:t+1}) | x_n^{1:t}(d_n^{1:t}), z_n]$. Under Assumptions 1 and 2, β_n is identifiable from A_n and b_n .

Proof. Let b_n be a $(T_{0_n} - 1) \times 1$ vector where each entry t is given by $\mathbb{E}[X_n^{t+1}(0^{1:t+1}) | x_n^{1:t}(0^{1:t}), z_n]$. We know from basic least-squares theory, and the given assumptions, that as long as the number $T_0 \geq r$ of observations is larger than or equal to the dimension r , the system is (over-)determined and $\beta_n = A_n^+ b_n$. □

Theorem 1 Assume we have a dataset of N units and T time points $(d_n^{1:T}, x_n^{1:T}, z_n)$ generated by a model partially specified by Eq. (1). Assume also knowledge of the conditional expectations $\mathbb{E}[X_n^t(d_n^{1:t}) | x_n^{1:t-1}(d_n^{1:t-1}), z_n]$ and basis functions $\phi_l(\cdot, \cdot)$ for all $l = 1, 2, \dots, r$ and all $1 \leq n \leq N$ and $1 \leq t \leq T$. Then, under Assumptions 1-4 applied to all individuals and all intervention levels d that appear in our dataset, we have that all β_n and all $\psi_l(d, \cdot, \cdot)$ are identifiable.

Proof. By Assumptions 1 and 2, and Proposition 3, all β_n are identifiable.

For the next step, let

$$\eta_{nl}^t := \beta_{nl} \times \prod_{t'=1}^t \psi_l(d_n^{t'}, t', t),$$

and

$$\alpha_{dl}^{\Delta t} := \prod_{t'=1}^{\Delta t} \psi_l(d, 1, t').$$

Consider now the first time t an intervention level $d > 0$ is assigned to someone in the entire dataset. By Assumption 3, there exists a dataset \mathcal{N}_d with the given properties where, for all $n \in \mathcal{N}_d$, we have $\eta_{nl}^t = \beta_{nl} \times \prod_{t'=1}^t \psi_l(d_n^{t'}, t', t) = \beta_{nl}$, since all interventions prior to t have been at level 0.

Let $b_{dt'}$ be a $N_d \times 1$ vector where each entry i is given by $\mathbb{E}[X_{n_i}^{t+t'}(d_{n_i}^{1:t+t'}) | x_{n_i}^{1:t+t'}(d_{n_i}^{1:t+t'}), z_{n_i}]$, for $t' = 1, 2, \dots, k_d - 1$. Consider the time-bounded case with free parameters $w_{dl,l}$, $l = 1, 2, \dots, r$. Given Assumption 4, we can solve for $\eta_n^{t+1} = A_{d_1}^+ b_{d_1}$, the vector with entries η_{nl}^{t+1} .

As $\eta_{nl}^{t+1} = \eta_{nl}^t \times \psi_l(d, t+1, t+1) = \eta_{nl}^{t+1} \times w_{dl,1}$, with non-zero η_{nl} by Assumption 3, this also identifies $w_{dl,1}$. Also by Assumption 3, at time point $t+2$ we have that $\eta_{nl}^{t+1} = \eta_{nl}^t \times \psi_l(d, t+1, t+2)$ for all units in \mathcal{N}_d , which by analogy to the previous paragraph, identifies $\psi_l(d, t+1, t+2)$ and consequently $w_{dl,2}$. As this goes all the way to $t+k_d-1$, this identifies all of $\psi_l(d, \dots, \cdot)$.

If intervention d level is the time-unbounded model of Eq. (3), by Assumption 3, we also identify α_d^1 , α_d^2 and α_d^3 , as they are defined by functions $\psi_l(d, t+1, t+t') = \psi_l(d, 1, t')$ for $t' = 1, 2, 3$ that we established as identified by the reasoning in the previous paragraph. As $\sigma(w_{1dl}) \times w_{2dl} - \sigma(w_{1dl})^2 \times w_{2dl} = \alpha_{dl}^1 - \alpha_{dl}^3$ and

$$\frac{\sigma(w_{1dl}) \times w_{2dl} - \sigma(w_{1dl})^2 \times w_{2dl}}{\sigma(w_{1dl})^2 \times w_{2dl} - \sigma(w_{1dl})^3 \times w_{2dl}} = \frac{\alpha_{dl}^1 - \alpha_{dl}^2}{\alpha_{dl}^2 - \alpha_{dl}^3},$$

solving for the above results in

$$\begin{aligned} w_{1dl} &= \sigma^{-1} \left(\frac{\alpha_{dl}^2 - \alpha_{dl}^3}{\alpha_{dl}^1 - \alpha_{dl}^2} \right), \\ w_{2dl} &= \frac{\alpha_{dl}^1 - \alpha_{dl}^3}{\sigma(w_{1dl}) - \sigma(w_{1dl})^3}, \\ w_{3dl} &= \alpha_{dl}^1 - \sigma(w_{1dl}) \times w_{2dl}. \end{aligned}$$

So far we have established identification of the $\psi(d, \cdot, \cdot)$ functions for the first intervention level d that appears in the dataset (the value d is not unique, as it is possible to assign different intervention levels d' in parallel at time t , but to different units). We now must show that, for the remaining interventions $d > 0$ levels take place in our dataset after time t .

Assume the induction hypothesis that t_s is the s -th unique time an intervention level $d > 0$ is assigned to some unit in the dataset, and all intervention levels d^* that appeared up prior to t_d have their functions $\psi_l(d^*, \cdot, \cdot)$ identified. We showed this is the case for $t_1 = t$, which is our base case. We assume this to be true for t_s and we will show that this also holds for t_{s+1} .

Let d be an intervention level assigned at t_{s+1} and let \mathcal{N}_d the corresponding subset of data assumed to exist by Assumption 3. For any $n \in \mathcal{N}_d$, let s_- be the last time a non-zero intervention d_- has been assigned to n prior to $s+1$. Also by Assumption 3, this must have taken place at least k_{d_-} steps in the past. By the induction hypothesis, $\psi_l(k_{d_-}, \cdot, \cdot)$ is identifiable, and therefore so is the case for all $\psi_l(k_{d_{\prec}}, \cdot, \cdot)$ for intervention levels d_{\prec} taking place for the first time prior to t_s . This also implies that $\eta_{nl}^{t_s}$ is identified, and the rest of the argument proceeds as in the base case. \square

Theorem 2 Assume we have N calibration samples,

$$S_n^{t'} = |X_n^{t'} - f(D_n^{1:t_n}, X_n^{1:t_n}, Z_n)|, \quad t' = t_n + \Delta < t, \quad n = 1, \dots, N \quad (30)$$

where t_n is the time user n experienced the last intervention before t . Assume there exists $\epsilon > 0$ such that, for all n ,

$$p_T(S_n^{t+\Delta}) = (1 - \epsilon)p_C(S_n^{t+\Delta}) + \epsilon p_\delta(S_n^{t+\Delta}), \quad (31)$$

where p_T and p_C are the (unknown) densities of the test and calibration distributions, p_δ is a bounded arbitrary shift density, and $p_{\min} = \min_{n=1, \dots, N} p_C(S_n^{t'}) > 0$. Then,

$$\text{Prob}(X_{N+1}^{t+\Delta} \in C) \geq 1 - \alpha - \frac{1}{p_{\min}} \frac{\epsilon}{1 - \epsilon}. \quad (32)$$

Proof. Let P_T and P_C be the joint distributions of $(X_n^{t'}, D_n^{t'})$ for $t' > t$ and $t' \leq t$ and $w_n^{t'} = \frac{p_T(X_n^{t'}, D_n^{t'})}{p_C(X_n^{t'}, D_n^{t'})}$. For any $t' > t$, we can estimate P_T by weighting the calibration samples with $w_n^{t'}$, $n = 1, \dots, N$, i.e.

$$P_T(X, D) \approx Z^{-1} \sum_{n=1}^N w_n^{t'} \mathbf{1}((X, D) = (X_n^{t'}, D_n^{t'})), \quad Z = \sum_{n=1}^N w_n^{t'} \quad (33)$$

Conditional on the calibration samples, the $(1 - \alpha)$ -th empirical quantile of $P_T(X, D)$ is

$$Q_T(1 - \alpha) = \inf_q \left\{ \left(Z^{-1} \sum_{n=1}^N w_n^{t'} \mathbf{1}(S_n \leq q) \right) \geq 1 - \alpha \right\} \quad (34)$$

$$= \inf_q \left\{ \left(\sum_{n=1}^N \left(\frac{w_n^{t'}}{Z} - \frac{1}{N} + \frac{1}{N} \right) \mathbf{1}(S_n \leq q) \right) \geq 1 - \alpha \right\} \quad (35)$$

$$= \inf_q \left\{ \left(\frac{1}{N} \sum_{n=1}^N \mathbf{1}(S_n \leq q) \right) \geq 1 - \alpha - \sum_{n=1}^N \left(\frac{w_n^{t'}}{Z} - \frac{1}{N} \right) \mathbf{1}(S_n \leq q) \right\} \quad (36)$$

$$\geq \inf_q \left\{ \left(\frac{1}{N} \sum_{n=1}^N \mathbf{1}(S_n \leq q) \right) \geq 1 - \alpha - \sqrt{N} \sqrt{\sum_{n=1}^N \left(\frac{w_n^{t'}}{Z} - \frac{1}{N} \right)^2} \right\} \quad (37)$$

$$= Q_C(1 - \alpha - \text{gap}) \quad (38)$$

where $\text{gap} = \frac{\sqrt{N}}{Z} \sqrt{\sum_{n=1}^N (w_n^{t'} - \mathbb{E}(w^{t'}))^2} = \frac{N}{Z} \text{Var}(w^{t'}) = \frac{\text{Var}(w^{t'})}{\mathbb{E}(w^{t'})}$, with $\mathbb{E}(w^{t'})$ and $\text{Var}(w^{t'})$ being the empirical mean and variance of w^t estimated on the N calibration samples. Under the theorem assumptions, we have $w_n^{t'} = (1 - \epsilon) + \epsilon \frac{\delta(S_n^{t'})}{p_C(S_n^{t'})}$. Then, $\mathbb{E}(w^{t'}) = 1 - \epsilon + \epsilon \frac{\mathbb{E}(\delta(S^{t'}))}{p_C(S^{t'})} \geq 1 - \epsilon$ and $\text{Var}^2(w^{t'}) = \mathbb{E}(w^{t'} - \mathbb{E}(w^{t'}))^2 \leq \epsilon^2 \text{Var}^2\left(\frac{\delta(S^{t'})}{p_C(S^{t'})}\right) \leq \frac{\epsilon^2}{(\min_S p_C(S^{t'}))^2} \text{Var}^2(\delta(S^{t'})) \leq \frac{\epsilon^2}{(\min_S p_C(S^{t'}))^2}$. The statement follows from

$$\text{Prob}(Z \leq a) \geq \text{Prob}(Z \leq b) \quad \text{if } a \geq b \quad (39)$$

and the Quantile Lemma on $S_{N+1}^{t+\Delta}$, which implies $\text{Prob}(S_{N+1}^{t+\Delta} \leq Q_C(1 - \alpha_*)) \geq 1 - \alpha_*$, where α_* obeys

$$\alpha_* = \alpha + \text{gap} \leq \alpha + \frac{\sqrt{\text{Var}^2(w^{t'})}}{\mathbb{E}(w^{t'})} \leq \frac{\epsilon}{\min_S p_C(S)} \frac{1}{1 - \epsilon}. \quad (40)$$

□

C Simulators

We design two different simulators: (1) a fully-synthetic simulator; and (2) a semi-synthetic simulator.

C.1 General Setting

The simulators serve as fully controllable oracles to allow us test the performance of causal inference problems. In particular, we have the following parameters:

- N : the total number of training users.
- M : the total number of testing users.
- T : the total number of steps in a time series.

- T_0 : the number of steps in a time series when the intervention is the “default” one ($D = 0$).
- K : the number of different interventions (so that $D \in \{0, 1, \dots, K - 1\}$).
- r : the size of latent variable dimensions.
- z_{dim} : the size of time invariant feature dimensions.
- I : the maximum number of non-zero intervention levels in a time series.

Whenever possible, we set the same random seeds of 1, 2, 3, 4, 5 to aid reproducibility of our results. For the fully-synthetic simulator, a different seed indicates that it is a different simulator (randomly drawn of simulator parameters based on this seed) and also reflects the randomness that comes from neural network parameter initialization and data splitting when training models. For the semi-synthetic simulator, the simulator parameters ϕ and β are learned from real world data, but we will need to also draw synthetic parameters for ψ . In both cases, using different random seeds can be considered to be drawing new problems where each has unique parameters.

C.2 Fully-Synthetic Simulator

The first simulator is purely synthetic where all parameters are randomly sampled from some pre-defined distribution. The overall data generation process exactly follows the model we specified in Section 2.

We aim to generate a synthetic dataset for training with the following parameters: $r = 5$, $T = 20$, $T_0 = 10$, $K = 5$, $N = 50000$, and $z_{\text{dim}} = 5$. We generate 200000 at first place, but only use the first 50000 samples for training. For testing our performance, we generate additional non-overlapping $M = 5000$ samples with the same parameters, but this time with $T = 25$. We make predictions on the last 5 time steps based on the first 20.

The intervention effect parameters are sampled from the following distributions, each with a size of $K \times r$. For $d = 1, 2$:

$$\begin{aligned} w_{1d} &\sim \mathcal{U}(1, 2) \\ w_{2d} &\sim \mathcal{U}(1, 2) \\ w_{3d} &\sim \mathcal{U}(2, 3). \end{aligned}$$

For $d = 3, 4$:

$$\begin{aligned} w_{1d} &\sim \mathcal{U}(-2, -1) \\ w_{2d} &\sim \mathcal{U}(-2, -1) \\ w_{3d} &\sim \mathcal{U}(-1, 0). \end{aligned}$$

We set $w_{1d} = 0$, $w_{2d} = 0$ and $w_{3d} = 1$ to reflect the “idle” or “default” intervention level $d = 0$. The values are designed to be symmetric along the default intervention value. We generate random time series $\{D_n^t\}$ based on the identification results in Section 2.2, with the following rules:

1. we have enough default-intervention points ($T_0 = 10 \geq r$, see Assumption 1).
2. for each unique unit, the same type of intervention action does not repeat (by sampling without replacement). We additionally assume at least $I > K/2$ (in this case, $I = 3$) of the interventions show up in each unit-level time series.
3. once a $d > 0$ intervention happens, there must be at least two consecutive $d = 0$ interventions (see Theorem 1).
4. in the test dataset, at prediction time, we assume an unseen intervention in the first 20 time series shows up at exactly 21, and then the time series has no intervention until the end. An example of this will be training $D = [0, 0, \dots, 1, 0, \dots, 0, 2, 0]$ of $T = 20$ and testing $D = [0, 0, \dots, 4, 0, \dots, 0, 3, 0] + [2, 0, 0, 0, 0]$ of $T = 25$.

We generate a time series $\{\psi_n^t\}$, based on Eq. 2, using the corresponding w_{1d}, w_{2d}, w_{3d} values. We generate $\beta_n \sim \mathcal{N}(\mu_n, \sigma_n)$ for each user, each with a size of $N \times r$, as follows:

$$\begin{aligned} \mu_n &\sim \mathcal{N}(0, 1) \\ \sigma_n &\sim \exp\{\mathcal{N}(0, 1)\}. \end{aligned}$$

We generate unit-specific covariates $\{Z_n\}$ with $z_{\text{dim}} = 5$ of size $N \times z_{\text{dim}}$, as:

$$Z_n \sim \mathcal{N}(0, 3).$$

This is then used to set up an initial X_n^0 (the initial starting point of the time series) with a random-parameter MLP with input dimension of z_{dim} and output dimension of 1. Finally, to create the synthetic time series $\{X_n^{0:T}\}$ (0 comes from the initial starting point), we randomly generate a neural network consisting of a single layer long-short term memory (LSTM) and a MLP to generate ϕ at each time step. We further compose ϕ with a sigmoid function so that it is bounded between $[-1, 1]$. We iteratively sample the $\{X_n^t\}$ points with the conditional mean from Eq 1 (based on $X_n^{0:t-1}$, Z_n , and $D_n^{1:t}$) plus a standard Gaussian additive error term at each step.

The outcome of this simulator gives us the following data: time series $\{X_n^{0:T}\}$, intervention sequence $\{D_n^{1:T}\}$ and covariates Z_n .

C.3 Semi-Synthetic Simulator

The second simulator is semi-synthetic, in the sense that the simulator parameters are learned based on real world data from the WSDM Cup, organised jointly by Spotify, WSDM, and CrowdAI⁴. The dataset comes from Spotify⁵, which is an online music streaming platform with over 190 million active users interacting with a library of over 40 million tracks. The purpose of this challenge is to understand users’ behaviours based on sequential interactions with the streamed content they are presented with and how this contributes to skip track behaviour, which is considered as an important implicit feedback signal.

For a detailed description of the dataset, please refer to Brost et al. [2019]. We created our simulator based on the “Test_Set.tar.gz (14G)” file. After unzipping the test data, we randomly chose a file named (“log_prehistory_20180918_00000000000.csv”) as our main data source. In our case, we only use the columns named: “session_id”, “session_position”, “session_length”, “track_id_clean”, and “skip_3”. Here, each unique “session_id” indicates a different sequence of interactions from an unknown user and the length of the interaction is denoted by “session_length”, where each step is denoted by “session_position”. The column “track_id_clean” indicates the particular track a user listen to at each position in the process. “skip_3” is a boolean value indicating if most of the track was played by the user. We assign the number of 1 if it is “True” and 0 otherwise. We use this value to create X_n^t later.

To process the data, we start by looking at the existing sequence lengths and we select the most frequent sequence length in the data (20) (the actual corresponding session sequence is 10), which counts for around 57.95% of the original file. After filtering, there are around 228, 460 unique sessions and 301, 783 unique tracks in the data. To further reduce the computational cost of constructing a very large session-track matrix, we randomly sample a sub-population of 6000 unique session ids, which then bring us to 26, 707 unique tracks. We build the session-track matrix where the entry value is the number of counts a particular track been listened over a particular session based on this sub-population. We apply singular-value decomposition (SVD)⁶ to this session-track matrix to get the session embeddings and track embeddings. For numerical stability reason, we save only the top 50 singular values and further normalize it using its mean and standard deviation. For track embeddings, we take the top 10 singular values after the normalization and assign them into 10 clusters, using constrained K -means to encourage equal-sized clusters⁷. Using these clusters, we create a new categorical variable F and its continuous counterpart $\phi(F)$, which respectively represent the corresponding cluster and its centroid vector based on the value of its associated “track_id_clean” entry. Next, we set X_n^t as the cumulative sum of the corresponding binary “skip_3” value over each unique “session_id” with added zero-mean Gaussian noise with standard deviation $1/2$. We keep the first 5 singular values for the session embedding normalization and consider them to be the session specific covariate Z . We save X , F , $\phi(F)$ and Z as separate matrices as the final output, which have shapes of 6000×10 , $6000 \times 10 \times 10$, $6000 \times 10 \times 10$ and 6000×5 , respectively.

To build a simulator, we define the following two processes:

$$P(F_n^t | F_n^{1:t-1}, X_n^{1:t-1}, Z_n) = \text{softmax}(f(F_n^{1:t-1}, X_n^{1:t-1}, Z_n)),$$

and

$$X_n^t = \phi(F_n^t)^\top \beta_n + \epsilon_n^t,$$

where $\phi(F_n^t)$ is the 10-dimensional embedding of categorical variable F_n given by the cluster centroid, and $\epsilon_n^t \sim N(0, \sigma_x^2)$.

⁴<https://research.atspotify.com/datasets/>

⁵<https://open.spotify.com/>

⁶<https://numpy.org/doc/stable/reference/generated/numpy.linalg.svd.html>

⁷<https://github.com/joshlk/k-means-constrained>

Function $f(\cdot, \cdot, \cdot)$ is modeled with a deep neural network consisting of a single layer GRU and a MLP, trained on the real F with cross entropy loss (as a likelihood based model). The second equation is trained on the real X with an ordinary least square (OLS) regression with a ridge regularisation term ($\alpha = 0.01$). Error variance is estimated by setting $\hat{\sigma}_x^2$ to be equal to the variance of the residuals. This defines a semi-synthetic model calibrated by our pre-processing of the real data.

We now need to define interventions synthetically, as they are not present on the real data. We choose $K = 5$ as the size of the space of possible interventions. We will define interventions in a way to capture the notion of changing the exposure of tracks in particular cluster k for particular user n at time t . Since the real data does not contain information regarding how interventions can influence the behaviour of Spotify users, similar to the simulator setup for the fully-synthetic one, we use 5 random seed to indicates different possible changes to the users behaviour in the Spotify platform.

The intervention effect parameters are sampled from the following distributions, each with a size of $K \times r$. For $d = 1, 2$:

$$\begin{aligned} w_{1d} &\sim \mathcal{U}(1, 1.5) \\ w_{2d} &\sim \mathcal{U}(1, 1.5) \\ w_{3d} &\sim \mathcal{U}(1.5, 2.0). \end{aligned}$$

For $d = 3, 4$:

$$\begin{aligned} w_{1d} &\sim \mathcal{U}(-1.5, -1) \\ w_{2d} &\sim \mathcal{U}(-1.5, -1) \\ w_{3d} &\sim \mathcal{U}(0, 0.5). \end{aligned}$$

We set $w_{1d} = 0$, $w_{2d} = 0$ and $w_{3d} = 1$ to reflect the “idle” or “default” intervention level $d = 0$. The values are designed to symmetric along the default intervention value. We generate random time series $\{D_n^t\}$ based on the identification results in Section 2.2 and the rules we adopted in the full-synthetic simulator in Appendix C.2. Notice that the above does not correspond exactly to the model class we discuss in Section 2, as the product of intervention ψ in Eq. 2 is multiplied to the softmax operation of $f(F_n^{1:t-1}, X_n^{1:t-1}, Z_n)$ and also to the $\phi(F_n^t)$.

We generate a synthetic dataset for training with the following parameters: $r = 10$, $T = 35$, $T_0 = 25$, $N = 3000$, and $z_{\text{dim}} = 5$ (note, we have the first 5000 for training, but only use the first 3000 samples are used for actual training, as we have additional experiments to check the influence of more training data points). For testing our performance, we generate additional non-overlapping $M = 1000$ samples with the same parameters, but this time with $T = 40$ for making predictions on the last 5 time series based on the first 35.

To sample data from this simulator, we take the initial state of X_n^0 and F_n^0 from the pre-processed data. We use the Z_n vector which comes from the real-world user embedding. Then we iterative generated the next F_n via categorical draw from the softmax output based on user embedding Z_n all previous F_n and X_n . Once a categorical value of F_n is drawn, we replace it with its embedding form $\phi(F_n)$ which is the centroid of its cluster. We use this $\phi(F_n)$ to generate X_n plus an additive Gaussian noise with zero mean and homoscedastic variance learned from data.

The outcome of this simulator gives us the following data: time series $\{X_n^{0:T}\}$, intervention sequence $\{D_n^{1:T}\}$ and covariates Z_n .

D More Results

In this section, we present more experimental results on our method. This includes: (1) the effect of choosing r ; (2) further examples of visualization and empirical examples.

D.1 Effect on Choice of r

The effect of different r is presented in Fig. 3, with $r = 5$ being the ground truth parameter which data is generated. We have also plotted the performance of our method under $r = 3$ and $r = 10$. We observed that when r is smaller than the ground truth, the model tend to under-fit the data with a slight higher MSE error. When r is bigger than the actual value, the MSE error can be further reduced but also at the same time results in very large variance. We also show that this can be mitigated with further regularization such as applying L_1 and L_2 terms during likelihood learning process.

The insight we drawn from this is that when apply our approach in real-world problems, we could potentially choose a higher r without much concern about what an exact value should be. Using a large r leads to higher variance but in general performs reasonable well compare with knowing the true r (recall that here $r = 5$). We also notice that applying regularization technique even when we know the right dimension of r can be beneficial, leading to more stable performance (with lower variance), but does not change much of the mean estimate as shown in Fig. 3. This maybe partially caused by the gradient optimization process when training the deep neural network. Hence, we claim that the main price to be paid for a large choice of r is that this makes data requirements stricter (such as the number of steps prior to the first intervention) in order to guarantee identification.

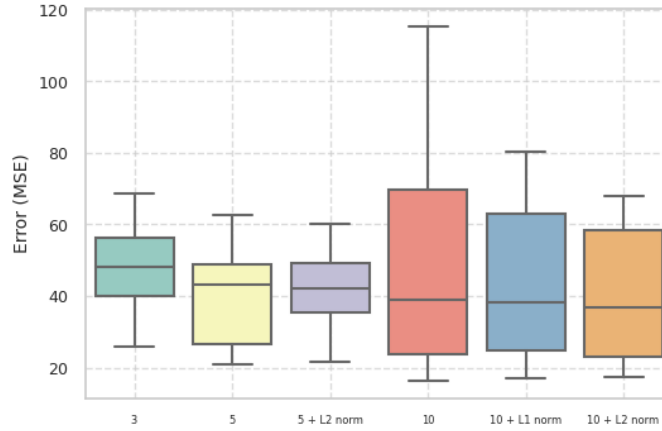


Figure 3: Effect of changing r for the fully-synthetic dataset.

D.2 Additional Figures

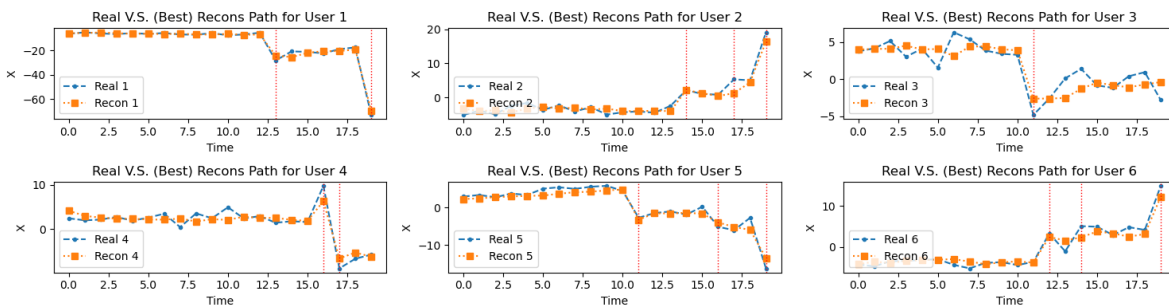


Figure 4: Examples of reconstruction of training data for CSI-VAE-1 model.

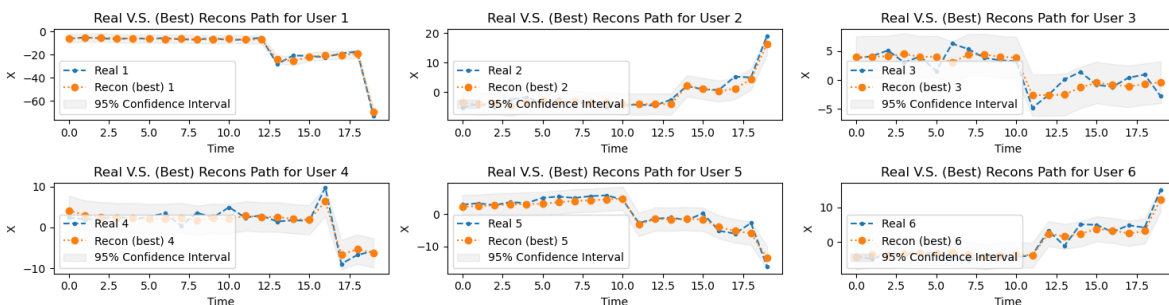


Figure 5: Model-based uncertainty quantification for Reconstruction (CSI-VAE-1).

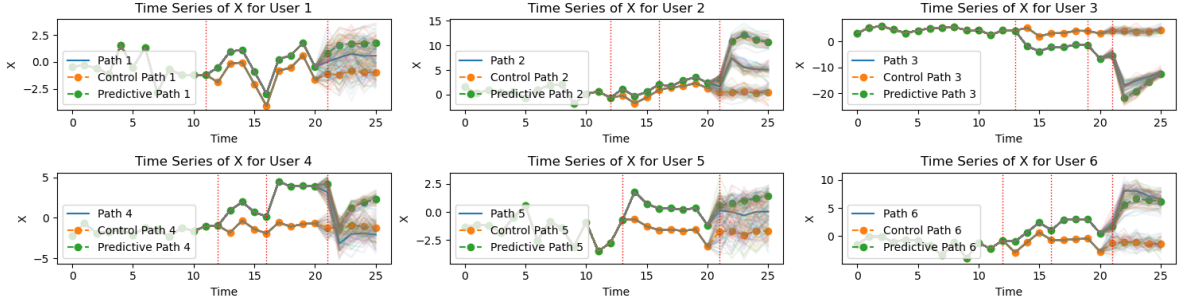


Figure 6: Demonstration of prediction for synthetic data for CSI-VAE-1.

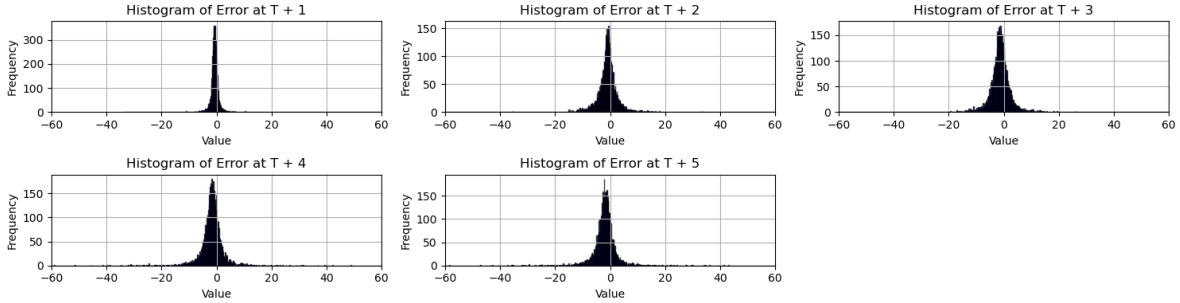


Figure 7: Residual distribution of our problems (based on CSI-VAE-1 model). In general, we observe a very long tail effect across model predictions.

E Uncertainty Quantification

For the sake of illustration, we generate another new dataset with a random seed of 42 using the synthetic simulator, based on the following specifications: $r = 5$, $T = 20$, $T_0 = 10$, $K = 5$, $N = 50000$, $z_{\text{dim}} = 5$, $I = 3$. We also generated two further datasets of $M = 2000$, one for calibration and one for test.

E.1 Plug-in Model-based Uncertainty Quantification

We first present the model based uncertainty quantification at level of $\alpha = 0.95$, in Fig. 8. Given our conditional mean and homoscedastic error variance σ^2 estimates from data, we can calculate predictive intervals as $(\mu - 1.96 \times \sigma, \mu + 1.96 \times \sigma)$. For purely model based uncertainty quantification with plug-in parameter estimates, we do not need an additional calibration dataset, but it is an obviously problematic one as it does not take into account estimation error and sampling variability. The coverage rate is 57.75% on the test dataset without further calibration.

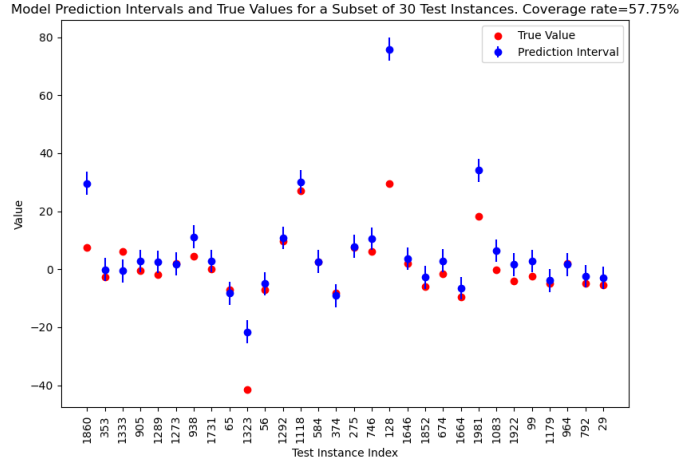


Figure 8: Plug-in model-based predictive interval and coverage.

E.2 Conformal Prediction

We then present the model-free uncertainty quantification at level of $\alpha = 0.95$ (based on the Setup 1 in section 3.2), shown in Fig. E.2. We use the absolute value over the predictive residual as our conformity score function, $\text{abs}(y - f(x))$. We calibrate our model output based on the calibration dataset and then apply it on the test dataset. We obtained a coverage rate of 95.30%. This is a significant improvement upon what we see in Fig. 8 and demonstrates the effectiveness of the conformal prediction approach.

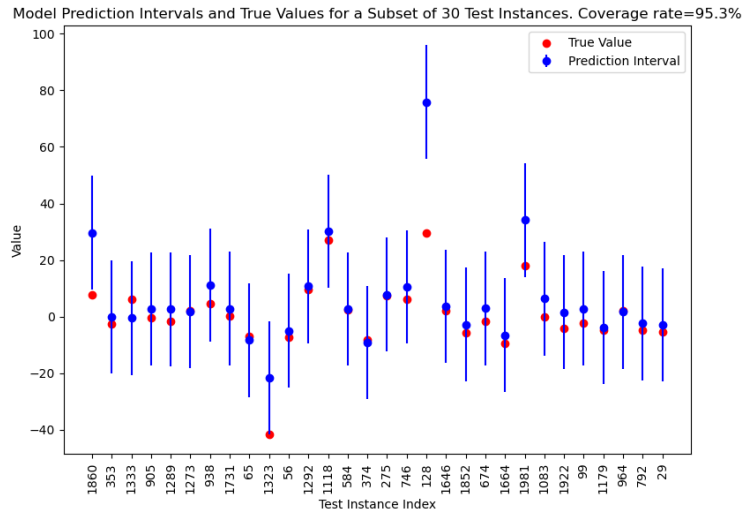


Figure 9: Conformal prediction predictive interval and coverage.